John H. Scofield, *Rev. Sci. Instrum.* **58** (6), June 1987, pp. 985-993.

AC METHOD FOR MEASURING LOW-FREQUENCY RESISTANCE FLUCTUATION SPECTRA

John H. Scofield
AT&T Bell Laboratories
Holmdel, NJ 07733

ABSTRACT

An ac technique is described for measuring low frequency resistance fluctuation spectra with improved sensitivity over dc methods achieved by avoiding preamplifier 1/f noise. The technique, easily implemented with decade resistors and a lock-in amplifier, allows the current noise of low resistance ($r < 10\ k\Omega$) specimens to be measured to frequencies below 1 mHz. Use of a center-tapped, four-probe specimen geometry allows discrimination between specimen and contact noise and eliminates noise due to bath temperature variations. The technique is demonstrated in use to determine the dependence of the 1/f noise of Cr films on film area. Measurements with simultaneous direct and alternating currents provide means to study the noise of nonlinear devices and frequency dependent conductors.

PACS: 72.70, 05.40, 73.60D
Date: 17-Feb-87

1. Background

1.1 Introduction

Fluctuations about equilibrium are generally interesting in that they convey information about system dynamics near equilibrium. Resistance fluctuations reflect the dynamics of the physical systems to which the conduction processes are coupled. For instance, resistance fluctuations of Sn films just above their superconducting transition reflect the dynamics of heat flow [1]. It has been suggested [2] and verified [3] that resistance fluctuations of thin metal films may probe the kinetics of chemisorption. Others have used resistance fluctuation spectra of Al films to probe vacancy creation/annihilation [4] and dislocation dynamics [5]. More recently resistance fluctuations of Nb films have been shown to reflect the dynamics of hydrogen diffusion [6].

Moreover, a wide variety of conductors exhibit a phenomenon known as "1/f noise," i.e., low frequency resistance fluctuations $\delta r(t)$ having power spectra $S_r(f) \propto 1/f^{\alpha}$, $\alpha = 1$ [7]. The apparent decrease of the relative noise magnitude $fS_r(f)/r^2$ with increasing conductor size makes it difficult to study the phenomenon in bulk materials, and accentuates the potential practical problem of 1/f noise in sub-micron conductors. In metals the 1/f-resistance fluctuations are so low in level that they have been measured only for thin films ($t \leq 100$ nm), whiskers [16], and point contacts whose properties are not necessarily those of the bulk material. Measurements are often perturbed by significant Joule heating due to the use of large measurement currents [8]. There has to date been insufficient sensitivity to measure the 1/f noise of metals at temperatures below 50 K [9,16]. The sensitivity of the dc four-probe method, which is usually used to measure resistance fluctuations, is limited by low frequency preamplifier noise.

Here, an ac method is introduced for measuring resistance fluctuation spectra with sensitivity limited, not by the low frequency preamplifier noise, but rather, by the preamplifier noise at the modulation frequency. The method is simply a wide-band adaptation of phase sensitive detection (PSD) techniques commonly employed with ac resistance bridges. The introduction of a five-probe conductor geometry makes it possible to eliminate contact noise while placing the sample in a Wheatstone bridge. A lock-in amplifier is used to amplify and demodulate noise sidebands produced by fluctuations $\delta r(t)$ of a center-tapped, four-probe resistor r in an ac Wheatstone bridge. The technique allows sub-mHz measurements of fluctuations of low resistance samples, not possible with dc methods. In contrast to the standard dc four-probe method which allows measurement of the noise power S_V as a function of two variables, the current I_o and frequency f, this ac method allows measurement of S_V as a function of five variables, f, current amplitude i_o, dc bias I_o, carrier frequency f_o, and phase detection angle δ (the current $I(t) = I_o + i_o \sin(2\pi f_o t + \delta)$). These additional parameters may prove useful in

understanding fluctuations in non-linear devices, frequency dependent conductors, and complex impedances.

Alternating-currnet measurements of 1/f-resistance fluctuation spectra have previously been reported [10-13] and several techniques have been proposed [14,15]. Previous ac measurements, however, have not eliminated contact noise (i.e., were two-probe), did not demodulate the carrier, and have required the building of specialized electronics. This five-probe method distinguishes specimen from contact noise and the only electronics required is a commercial lock-in amplifier. Furthermore, since the lock-in amplifier's PSD demodulates the signal, the spectrum of the output may be analyzed exactly as for the usual dc measurement.

In the remainder of this section the standard dc four-probe noise measurement will be described and its limitations enumerated. Section (2) describes successive modifications that remove these limitations, finally arriving at the subject of this paper, the five-probe ac bridge method. Section (3) describes the physical realization of the five-probe ac bridge method which is then used in section (4) to measure the 1/f noise of various conductors. In section (5) a number of other measurements are briefly described.

1.2 Four-probe dc noise measurement

The standard dc four-probe method for measuring resistance fluctuations is illustrated in Figure 1 [8,16,17]. A constant current $I = I_0 = E_0/R$, established by a stable battery E_0 in series with a large, stable ballast resistance $R \equiv R_1+R_2$ flows through the current leads of a fluctuating specimen resistance $r(t) \equiv \bar{r} + \delta r(t)$ (see Figure 2). The specimen resistance $r \equiv r_1 + r_2$ is broken into halves for later comparison with bridge methods. The average voltage $\langle v \rangle = I\langle r \rangle$ is removed by a dc blocking capacitor C (i.e., a high pass filter) so that fluctuations $\delta v(t) \equiv v(t) - \bar{v}$ in the voltage drop v across the specimen may be amplified and measured. The effect of fluctuations in the current contact resistances ξ_1 and ξ_2 (i.e., contact noise) is reduced by choosing R/r>>1. For sufficiently large R/r (see Appendix A) the power spectrum $S_V(f;I_0)$ of the voltage $\delta V(t)$ at the preamplifier output is

$$S_V(f;I_0) \approx G^2\left[S_v^0(f) + I_0^2 S_r(f)\right] \qquad (1)$$

where $S_r(f)$ is the power spectrum of $\delta r(t) \equiv \delta r_1(t)+\delta r_2(t)$, $S^o_v(f)$ is the power spectrum of the background noise (amplifier + thermal noise), and G is the preamplifier voltage gain. The excess noise $S_V(f;I) - S_V(f;0)$ should be measured for at least two different values of the ballast resistance R to determine whether the current is sufficiently constant to eliminate contact noise. Independence of calculated $S_r(f)$ on the ratio R/r is proof that the contact noise has been eliminated [16].

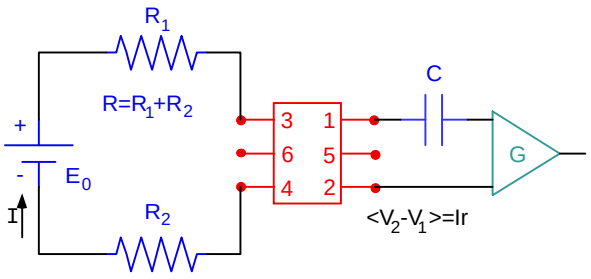

Figure 1. Circuit for the usual four-probe noise measurement. The six-probe device is the noise specimen of Figure 2. The ballast resistance R is split into two equal pieces R_1 and R_2 for comparison with the five-probe bridge noise measurement.

(a)

The above four-probe dc method has several limitations, especially when applied to low resistance conductors (e.g., metal films). First, measurements are limited to frequencies above the R_AC knee of the blocking capacitor C and amplifier input impedance R_A. Secondly, fluctuations δE in the battery voltage show up directly in the measured noise, prohibiting the use of power supplies. Thirdly, the sensitivity is limited by $S^o_v(f)$, which at low frequencies is dominated by preamplifier 1/f noise, which greatly exceeds the intrinsic thermal noise. While an impedance matching transformer may be used to reduce this latter problem its frequency response will then typically limit measurements to frequencies above 1 Hz.[19] And finally, one must always worry about thermoelectric effects, electromigration, and resistance fluctuations associated with bath temperature fluctuations.

2. Measurement Improvements

2.1 DC Bridge

The use of a bridge circuit to remove the average voltage drop $I\langle r \rangle$ avoids the first two limitations mentioned above [17]. There are a variety of ways to place a four-probe resistor in a Wheatstone bridge. In each case contact noise may be eliminated only at the expense of increasing the input impedance (seen by the preamplifier) and thus the background noise.

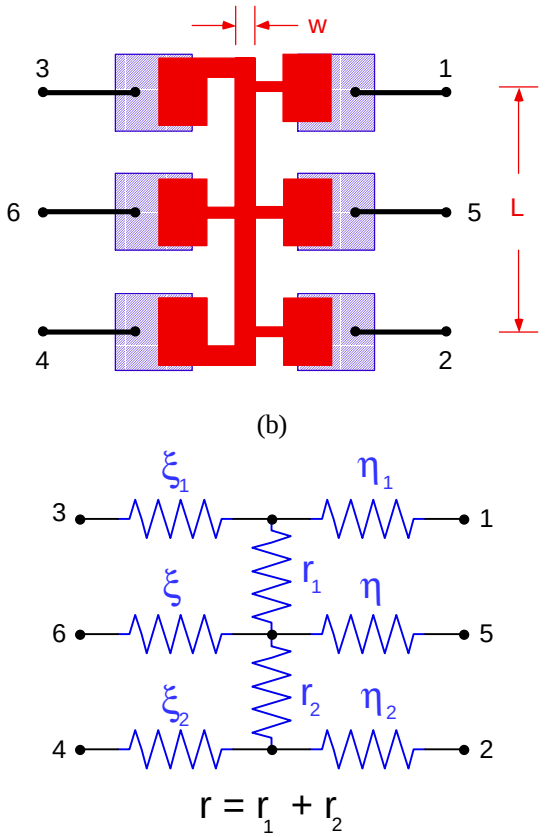

Figure 2. Detail of the multi-probe noise specimen. (a) Geometry, and (b) equivalent circuit. The usual four-probe resistance $r \equiv r_1 + r_2$ (with $r_1 \approx r_2$) of width w and length L is obtained by ignoring the center contacts (3 and 6).

This problem may be avoided by using a symmetric four-probe resistor with center tap as shown in Figure 3 [18]. When balanced, the bridge error signal is insensitive to fluctuations δE in the supply voltage or, equivalently, to fluctuations in the center contact resistance, ξ. As with the standard four-probe measurement large ballast resistors R_1 and R_2 reduce the effect of fluctuations in the current contact resistances, ξ_1 and ξ_2. In the limit $R_j/r_j >> 1$ (j=1,2) the input impedance to the preamplifier is r (thus the background noise $S^o_V(f)$ is the same as with the standard four-probe method) and the measured voltage spectrum is

$$S_V(f;I_0) \approx G^2\left[S_v^0(f) + I_0^2 S_r^-(f)\right] \qquad (2)$$

where $S^-_r(f)$ is the power spectral density of the difference $\delta r_-(t) \equiv \delta r_2(t) - \delta r_1(t)$. This has the added advantage of rendering the measurement insensitive to bath temperature fluctuations. If $\overline{\delta r_2 \delta r_1} = 0$ then $S^-_r(f) = S_r(f)$ and the measured spectrum is the same as before. If δr_2 and δr_1 are correlated, as is the case for noise associated with hydrogen diffusion in Nb films then $S^-_r(f)$ and $S_r(f)$ may differ significantly [6].

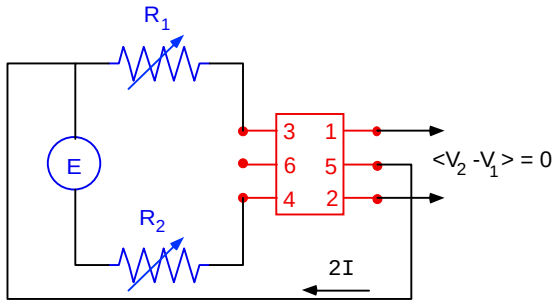

Figure 3. Circuit for the bridge measurements. The six-probe device is the noise specimen of Figure 2.

2.2 Background and Preamplifier Noise

While the bridge arrangement improves upon the standard four-probe method, the sensitivity is still limited at low frequencies by preamplifier noise [19]. This is best illustrated with a specific example. Consider the background noise of a r = 100 Ω resistor in a dc bridge arrangement measured with a Princeton Applied Research (PAR) model 113 low-noise preamplifier. The intrinsic thermal noise, 4kTr = 1.6×10^{-18} V^2/Hz, is indicated by the horizontal solid line in Figure 4. The actual measured noise (corrected for a $G = 10^4$) is plotted as curve (a) in the same figure. At high frequencies the background noise exceeds the thermal noise by more than 15dB, and only gets worse at lower frequencies. Since the 100 Ω sample resistance is poorly matched to the 100 MΩ input impedance of the preamplifier, an impedance matching transformer may be used to give (in principle) noise-free voltage gain before the preamplifer [19].

Figure 5 summarizes the noise added by a PAR 113 preamplifier for various input impedances and frequencies.[20] The noise figure (NF) of the amplifier is a measure of the amount of noise (referred to the input) added by the amplifier over and above the thermal noise of the impedance at its input *at room temperature;* $NF(f,r) = 10dB\log_{10}\{S^o_V(f)/4kT_or\}$, where $T_o = 290K$. The horizontal dashed line for a source resistance of 100 Ω represents the typical amplifier noise for this dc measurement; these same data give the upper dashed curve in Figure 4. The dashed curve and measured background noise (curve (a)) dissagree simply because the noise figure contours of Figure 5 are not actually measured from the preamplifier used, but rather are "typical."

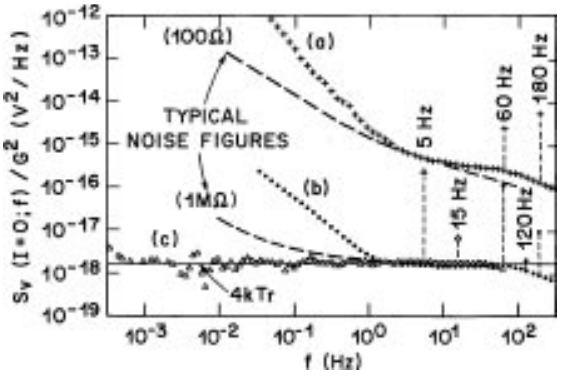

Figure 4. Background noise measurements with a 100 Ω load resistance using a PAR 113 preamplifier. Curves (a) and (b) are the measured dc background noise; (a) is measured with the preamplifier directly while (b) is measured with a PAR 190 impedance matching transformer and preamplifier. The two dashed curves represent the expected background noise for these measurements (based on manufacturer's "typical" noise figure contours) for an input impedance of 100 Ω (direct coupled) and 1 MΩ (transformer coupled). Curve (c) is measured at the output of the lock-in amplifier (reference at 65 Hz) and illustrates the background noise using the ac technique.

The PAR 113 NF contours show a minimum (called the "eye") near a source resistance r_e= 1MΩ and a frequency of 100 Hz. An impedance matching transformer with turns ratio $(N_2/N_1)^2 = r_e/r$ may be used to shift the operation of the PAR 113 with a 100 Ω bridge to the 1MΩ horizontal line (see Figure 5); these data give the lower dashed curve in Figure 4. The measured background noise using a PAR 190 (100:1) low-noise transformer before the preamp (total gain = $10^4\, N_2/N_1 = 10^6$) is plotted as curve (b) in Figure 4. Note that the transformer adds some noise of its own, much of which may be eliminated by magnetic shielding, vibration isolation, and cooling the transformer [21]. Properly impedance matched, the background noise approaches the thermal noise between 1 and 100 Hz. Below 100 mHz the frequency response of the transformer (not shown) drops to zero so that it is no longer useful. The roll-off above 100 Hz is also do the frequency response of the transformer. A flatter frequency response may be obtained by slightly mismatching the impedances of the bridge and PAR 113, but at the expense of additional preamplifier noise. The trade-off is usually worth it for room temperature measurements, but may not be if the sample is cold.

2.3 AC Bridge With Phase Sensitive Detection

Impedance matching allows the preamplifier to be used at its optimum input impedance. However, to measure resistance fluctuations down to zero frequency the preamp must still be used far away from its optimum frequncy. While cross-correlation techniques can reduce preamplifier noise their use below 1 Hz is limited [22]. An ac technique overcomes this difficulty by shifting the frequency at which the preamplier is used from zero (dc) up to the carrier frequency f_o [10]. With an alternating current $I = i(t) \equiv i_o \sin(2\pi f_o t)$ the resistance fluctuations modulate the carrier to produce noise sidebands. The preamplifier will contribute little noise in a bandwidth Δf if f_o is chosen within the eye of its NF contours. After amplification the carrier is demodulated to retrieve the desired low frequency resistance fluctuations. The point is that an ac current allows the preamplifier to be used near its optimum frequency. The lock-in amplifier was designed to perform precisely this function.

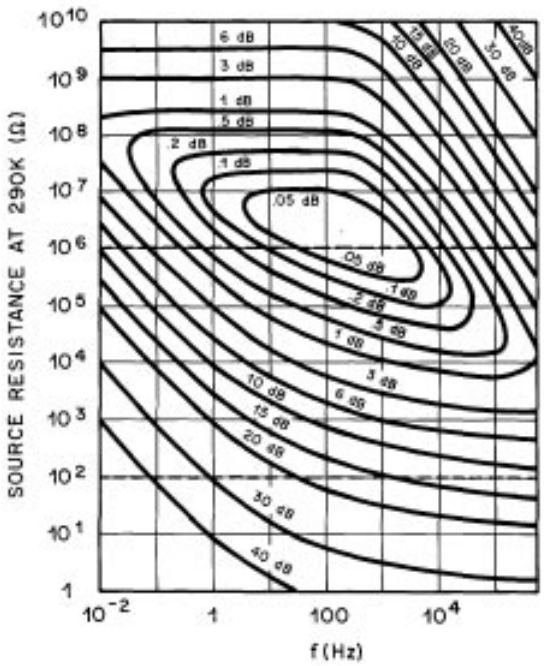

Figure 5 Typical noise figure contours for the PAR model 113 low noise preamplifier. The horizontal dashed lines represent expected preamplifier noise levels when used directly (100 Ω) and with a 100:1 impedance matching transformer (1 MΩ) with a load resistance of 100 Ω (see text).

Let the voltage source in Figure 3 be $E(t) = e_o \sin(2\pi f_o t)$. For a sufficiently low carrier frequency f_o capacitance effects may be neglected so that the bridge error signal is approximately $\delta r_j(t) i_o \sin(2\pi f_o t)$, where $i_o = e_o/(R_j + r_j)$ (j=1,2). The bridge error signal is inserted into the signal input of a lock-in amplifier with detection at a phase angle δ with respect to the bridge current. A block diagram of the set-up is shown in Figure 6. For frequencies $f < f_o/2$ the power spectral

density $S_V(f;i) \equiv S_V(f;i_o,f_o,\delta)$ of the output $\delta V(t)$ of the lock-in amplifier is (see Appendix B)

$$S_V(f;i) \approx G_0^2\left[S_v^0(f_0) + \tfrac{1}{2} i_0^2 S_r^-(f)\cos^2\delta\right] \qquad (2)$$

where the lock-in gain G_o is defined to be the ratio of the (dc) phase sensitive detector output voltage to the rms-voltage at the input. The principal improvement of the ac technique over the dc method is in the low frequency background noise, $S_V(f=0;i=0)/G^2_o = S^o_v(f_o)$. If f_o is chosen to be in the eye of the preamplifier's noise figure contours then at room temperature, $S^o_v(f_o) = 4kTr$. Note that both current noise and background (mostly thermal) noise are present at zero phase ($\delta = 0$) while just background noise is present when $\delta = 90$ A [23]. It is important to keep in mind that this technique does not lower the noise of a preamplifier, it only describes how to optimally use an arbitrary preamplifier for making low-frequency resistance fluctuation measurements.

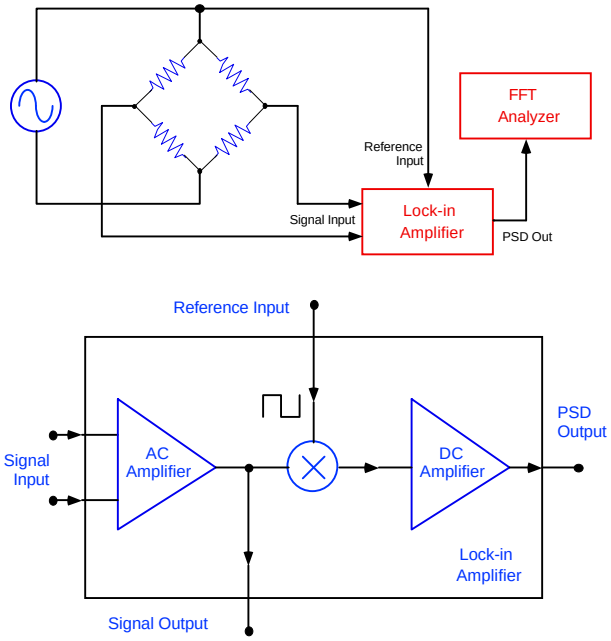

Figure 6 a) Block diagram of the experimental set-up using the lock-in amplifier to amplify and demodulate the bridge error signal. (b) Block diagram of the functions performed by the lock-in amplifier. The PSD demodulates the carrier by multiplying the output of the preamplifier by a square wave at the reference frequency.

The above ideas are illustrated with ac measurements of the background noise of the same 100 Ω resistor. The output of the same PAR 113/190 combination used earlier was fed into the input of a PAR 124 lock-in amplifier [24]. The lock-in was operated at low gain in its flat-band mode with a minimum time constant at the PSD output. A reference frequency of 65 Hz was chosen since it lies roughly in the middle of the low-noise, flat frequency response region of the preamp/transformer combination (see curve (b) of Figure 4). The resulting background noise spectrum is plotted as curve (c) in Figure 4. Measurements agree exactly with the dc transformer measurements in the frequency range 1 Hz to 50 Hz as they must. More importantly, the ac background noise is dominated by the specimen thermal noise down to the lowest frequency measured, 1 mHz. The spikes at 5 Hz and 15 Hz appear after multiplying 60 Hz and 180 Hz signals by a 65 Hz square wave during demodulation. To reduce this and to avoid other unwanted signals the lock-in should be used in its band pass mode so that negligible signal reaches the PSD at frequencies greater than $2f_o$. Note that one should verify that the input of the PSD does not contain significant signals that will be mixed to dc by the higher harmonics of the PSD square wave (see Appendix B).

3. Implementation of Five-probe AC Method

3.1 Instrumentation

The original realization of this technique used a parallel combination of 1.000 KΩ and 10.000 KΩ, non-inductively wound, 5-watt, 2 ppm/°C stable PRC (Precision Resistor Corporation) resistors mounted in large aluminum heat sinks for ballast resistor R_1. Ballast resistor R_2 was similarly formed but with a GenRad model 1433 decade resistor providing the (nominally) 10 KΩ shunt. The entire bridge was enclosed in an aluminum box surrounded with 2-in. styrofoam on all sides. Subsequent adaptations of the technique have used two rack mounted GenRad 1433 decade resistors for R_1 and R_2, trading stability for versatility. To achieve 1 ppm bridge balance at $f_o = 700$ Hz it was necessary to shunt R_2 with NP0 trimmer capacitors of a few hundred pF.

Bridge current was supplied either by the lock-in itself or by a Hewlett-Packard (HP) 3325A frequency synthesizer, typically operated at 700 Hz. In some cases a Kepco operational power supply was used after the synthesizer to provide a very low impedance voltage source. The bridge error signal (v_2- v_1) was fed into either a PAR 118 ($100\ \Omega \le r \le 3$ KΩ) or a transformer coupled PAR 116 preamplifier ($1\ \Omega \le r \le 300\ \Omega$) plugged into a PAR 124A lock-in amplifier operated in its bandpass mode with Q = 1. The lock-in's own low pass filter was usually set to have minimum effect. The output of the lock-in was passed

through a Unigon model LP-120, 120 dB/octave low-pass filter (cut-off frequency set to 500 Hz). In some cases a Krohn-Hite model 3320 high-pass filter (with corner frequency set to either 1 mHz or 10 mHz) was used to block slow drifts. The filtered output was fed into an HP 5420A spectrum analyzer, or into a Racal STORE-4DS FM data recorder for later analysis.

Choice of circuit ground has significant practical implications. Unless the current source is battery operated it will generally stipulate a circuit ground, say at sample pin 5 (see Figure 3). The bridge error signal, v_2-v_1, must then be connected differentially to the lock-in amplifier. This has the disadvantage of requiring significant common-mode rejection of the lock-in amplifier, sometimes exceeding its capability. If the contact resistance ξ is significant, as it frequently has been, this increases the common-mode signal and means that voltages v_1 and v_2 do not directly measure r_1 and r_2. This choice of circuit ground does, however, allow the current source to furnish both a direct and alternating currents, useful for some measurements.

Alternatively the oscillator may be transformer coupled to the bridge allowing arbitrary placement of circuit ground. In this case one convenient choice is to ground v_1 so that the lock-in does not see a common-mode signal at all. Unfortunately the lock-in then cannot measure r_1 or r_2 directly. A reasonable compromise is to ground here-to-for unused pin 6 of the sample. This eliminates any voltage dropped across ξ_1 from the common-mode signal at the preamplifier while allowing v_1 and v_2 to directly measure r_1 and r_2 respectively. An alternate scheme using a third bridge leg connected to sample pin 6 has been used [25].

3.2 Specimen Preparation

The five-probe ac method has been used to measure resistance fluctuations in thin continuous metal films. Highly polished, 0.010" x 1/2" x 1/2" sapphire substrates (obtained from Adolf Meller Co.) were prepared with a gold contact layer by evaporating 20 nm of Cr followed by 300 nm of Au through a CuBe deposition mask held 0.003" from the substrate. Noise specimens were subtractively patterned from another metal film, either sputtered or evaporated onto the substrate and gold contacts. Standard photolithographic techniques were used to form patterns in AZ1350J resist for four or five, six-probe specimen resistors with large connecting contact pads that overlapped the gold contact layer shown in Figure 2(a). Resist patterns were subsequently transferred to the metal film by chem- or sputter-etching, the latter accomplished in a non-reactive Ar^+ plasma. Specimen widths (w) and lengths (L) were measured with a calibrated optical microscope; they agreed with photomask dimensions except for the narrowest chem-etched specimens. Film thicknesses (h) were 1) monitored with a quartz crystal monitor during depositon, 2) measured with an Alpha-Step stylus, and 3) inferred from the measured residual resistivity ratios (RRR) combined with tabulated bulk resistivities. Resistances r_1 and r_2 of the specimen halves seldom differed by more than 5%. Finished substrates were mounted with Apiezon N-grease onto 24-pin, gold plated, nickel hybrid packages (Hermitite model MP-7777-24-3) and 0.7 mil $Au_{0.99}IN_{0.01}$ wires ultrasonically bonded between the Au contact layer and the package. In some cases it was possible to eliminate the Au contact layer altogether by ultrasonically bonding 1.5 mil $Al_{0.99}Si_{0.01}$ wires between the package and the specimen contact pads.

4. Experimental Results

The insensitivity of the bridge balance to fluctuations in specimen temperature is illustrated by low temperature measurements of the excess noise of carbon resistors. Two carbon composition resistors and two large commercial metal film resistors were placed in a temperature scanning dewar, wired so that any two could be used in the Wheatstone bridge as specimen resistors r_1 and r_2. The 1/f noise and temperature coefficents of resistance of the carbon resistors far exceeded those of the metal film resistors. The excess noise observed with one metal film resistor and one carbon resistor at 10 Kelvin is plotted as curve (MC) in Figure 7; it is entirely due to resistance fluctuations in the carbon resistor. Above 1Hz the 1/f noise of the carbon resistor dominates while below 1Hz the noise is due to fluctuations in bath temperature. The excess noise of the two carbon resistors is plotted as curve (CC) in the same figure. In this case the temperature fluctuations cancel, leaving just the 1/f noise, a factor of two greater than before due to the addition of two uncorrelated 1/f noise sources. Since thermal relaxation times are proportional to heat capacities (in this case of the copper specimen holder) which decrease with temperature, the knee in the spectrum of (MC) moves to higher frequency with decreasing temperature. With the usual four-probe measurement this effect could easily give an impression of a steeper slope in the spectrum with decreasing temperature, as has been reported for continuous metal films [9].

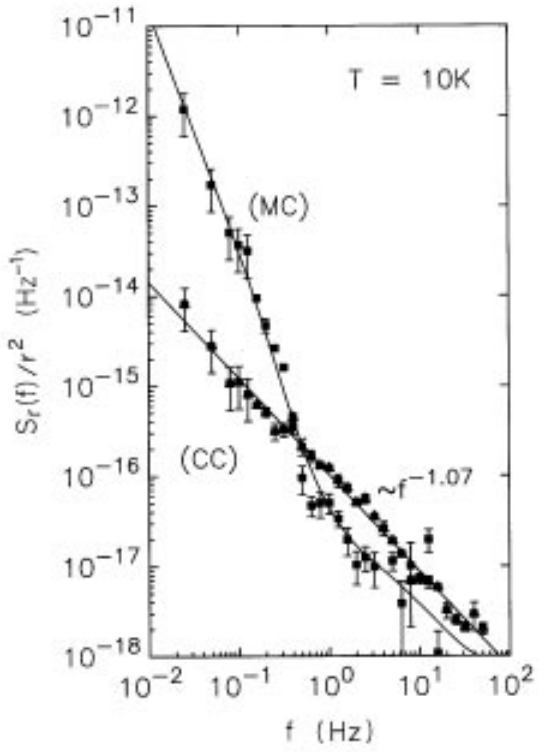

Figure 7. Noise measurements in the presence of bath temperature fluctuations. The solid lines are guides to the eye. (MC) Excess noise from a carbon resistor (= r1) and a commercial metal film resistor (= r_2) at T=10K (see text). (CC) Excess noise from two matched carbon resistors measured under similar conditions.

The ac technique has been used to measure room temperature 1/f noise from more than 60 continuous metal film specimens from 23 depositions of Ag, Al, Au, Cr, Cu, Ni, Mo, and W [26] At sufficiently low current levels the excess noise $\{S_V(f;i) - S_V(f;0)\} \propto i^2_o$. At higher current levels stronger current dependences were sometimes observed accompanied by instabilities in the bridge balance. They are thought to be associated with Joule heating and may be conveniently recognized and avoided by attention to bridge stability. With isolated exceptions the 1/f noise of specimens prepared from films of a given deposition were found to be reproducible to within about 30% [27]. Moreover, with similar precision the 1/f noise spectra $S^-_r(f)$ of specimens (differing only in length L and width w) are found to vary inversely with their area, A = Lw. This is illustrated by the excess noise of four specimens prepared on the same substrate from a (120±20) nm thick Cr film of resistivity ρ = (115±20) μΩcm. The size-normalized, relative resistance fluctuation spectra, $N_a S^-_r(f)/r^2$, for these four specimens are plotted in Figure 8, each with a different symbol. (N_a is the number of atoms in the specimen volume Ω = Lwh.) The figure clearly shows that, at all frequencies, the normalized spectra differ by no more than 50 % while the areas (Lw) vary by a factor of 200. The inset of Figure 8 shows a log-log plot of the relative noise level $\{fS^-_r(f)/r^2\}_{f=1Hz}$ versus N_a. A least-squares fit to the four points gives a slope of -1.05, not significantly different from a −1.0 slope. The same behavior has always been observed for other sets of specimens with the area commonly varying by a factor of 16. These results are so consistent that checking for an A^{-1} dependence serves as a useful test to eliminate noise due to extraneous sources like bath temperature fluctuations. It should be noted, however, that these data are in no way evidence for a bulk noise origin since both the surface area and volume vary together. Evidence distinguishing bulk from surface origins is obtained only by varying the film thickness (i.e., the surface to volume ratio) [28]. The w^{-1} dependence here places an upper limit of about 1 μm on the correlation length of the local resistivity fluctuations in the frequency range considered. We have not experienced the factor of two to ten irreproducibility reported by other laboratories [9,29].

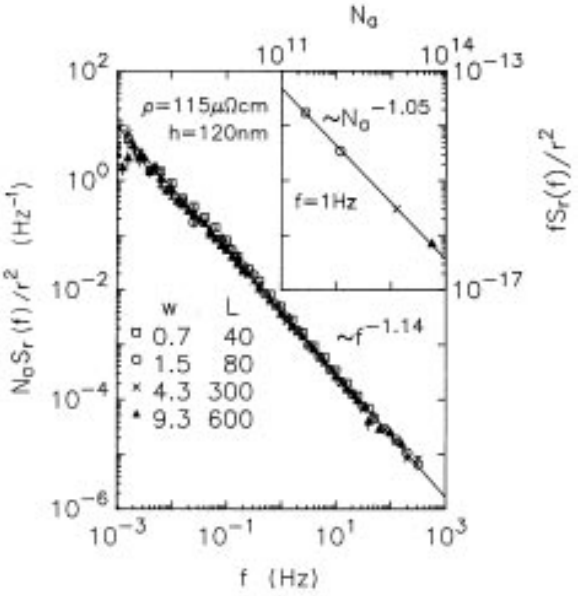

Figure 8. Log-log plots of the size-normalized relative resistivity fluctuation spectra of four Cr specimens fabricated from the same film. The symbols, lengths L (in μm), and widths w (in μm) are tabulated in the figure. The figure inset is a log-log plot of the relative noise level $\{fS_r(f)/r^2\}_{f=1Hz}$ versus specimen size (N_a). The distance between either voltage probe and the center contact is L/2. In practice $r_1 = r_2$ and $R_1 = R_2$; the specimen resistance $r \equiv r_1 + r_2$.

The 1/f noise of a metal film was never found to depend on the carrier frequency f_o nor was significant excess noise observed for $\delta = 90°$. The carrier frequency was systematically varied between 80 Hz to

5 KHz for one gold film; measurements agreed with each other, and also with the results of a dc five-probe bridge measurement. Results for an Al specimen were typical of out-of-phase noise measurements. In this case the power spectrum of the out-of-phase excess noise was less than 1/100th the level of that of the in-phase excess noise.

Some lock-in amplifiers (e.g., PAR 124A) may be operated in a flat frequency response mode and the amplified signal monitored both at the input and output of the phase-sensitive detector (i.e., before and after demodulation). With a direct bridge current I_o the PSD-input may be spectrum analyzed to obtain the dc five-probe measurement of Eq.(2). With a bridge current $I_o+i_o\sin(2\pi ft+\delta)$ the spectrum of Eq.(2) is available at the PSD-input while the spectrum of Eq.(3) is available at the PSD-output. These two signals have been used to cross-correlate the 1/f noise and 1/Δf-noise [12] of two matched 50 Ω carbon resistors (similar to those of Figure 7). With a 500 Hz carrier frequency f_o the measured coherence [30] $\gamma^2(f)$ between the two signals reaches a peak value $\gamma^2(5\text{Hz}) = 0.9975$ falling either side to values of $\gamma^2(256\text{Hz}) = 0.975$ and $\gamma^2(2\text{Hz}) = 0.984$. The decreased coherence at the low frequency end is expected due to the presence of preamplifier 1/f noise and the fact that the lock-in preamplifier is ac coupled to its input. $\gamma^2(f)$ is also expected to decrease at higher frequencies where the two signals are dominated by thermal noise. The results are completely consistent with those reported by Jones and Francis [12].

5. Discussion

Several groups have reported observations of unrectified 1/f noise from resistors passing an alternating current [31-34] while others have detected noise sidebands about harmonics of the carrier [35]. More recent efforts have failed to confirm these reports [36] Such effects suggest non-linear mechanisms; a simple model involving diodes and resistors has been suggested [37]. As mentioned earlier, all previous ac noise measurements have used only two probes and have been subject to contact noise. It is easy to imagine that some rectification would take place at the contact interface between two materials. Such effects have not been observed with five-probe ac measurements on metal films.

The Cornell group has performed measurements on tunnel junctions with slightly non-linear I-V characteristics [38]. Preliminary results suggest that complicated I_o dependences of $S_V(f;I_o)$ measured with a direct current I_o resolve into simpler i_o and I_o dependences of $S_V(f;I)$ determined by ac measurements. The junctions show noise sidebands about the carrier's second harmonic, easily measured with the "$2f_o$" reference mode of the lock-in.

In principle, this ac technique may be used to study the excess noise of any resistance. However, preamplifier 1/f noise tends to be most problematic for low resistance samples. Moreover, stray capacitances complicate analysis for high resistances. The circuit acts like a simple ac resistance bridge as long as $2\pi f_o\tau << 1$. With $r = 100\ \Omega$ the bridge tends to become unstable for $f_o > 10$ KHz; dc noise measurements are preferred for $r > 10\ \text{K}\Omega$.

Proper impedance matching and choice of carrier frequency allows resistance fluctuations to be measured down to 1 mHz frequency with preamplifier noise minimized. With the PAR 116 preamplifier this amounts to no more than a 0.05 dB NF at 1 KHz, or 1% of the room temperature thermal noise of the sample resistor. In principle this can be accomplished with a PAR 190 low-noise transformer for $0.1\ \Omega \le r \le 10\ \text{K}\Omega$. As the sample temperature decreases the preamplifier noise becomes more important. Assuming a 0.05 dB NF and neglecting the temperature dependence of r, the preamplifier noise would become equal to the sample thermal noise at T = 3K. With transformer coupling, however, the thermal noise of the transformer winding resistances dominates well above 3K. This problem may be eliminated (achieving the 3K noise temperature) by cooling the transformer [21]. For large bridge currents the sensitivity may also be limited by the thermal stability of the bridge components and temperature drifts. For instance, with 50 Ω wire-wound resistors for r_1 and r_2 and $R_1 = R_2 = 500\ \Omega$ we found that $S_v(f;i)$ exceeded $S_v(f;i=0)$ at f = 10 mHz and i_o = 28 mA.

If contact noise is not important (as for inherently two-probe devices like tunnel junctions) the specimen resistor may be placed in just one arm of the bridge (say r_1). To reduce the effect of bath temperature fluctuations a "pseudo" five-probe device may be constructed from two matched devices (as was done for carbon resistors). If contact noise is to be eliminated, however, the symmetric four-probe specimen must be used. Note that the center contact ξ must be external to the bridge and that r_1 and r_2 must not be separated by any contact resistances. This cannot be achieved by connecting two separate four-probe devices together.

6. Conclusions

An ac technique for measuring resistance fluctuation spectra of low resistance conductors to sub-

mHz frequencies has been presented that is readily implemented with decade resistors, a lock-in amplifier, and a spectrum analyzer. Improved low-frequency sensitivity over dc methods is achieved by avoiding preamplifier 1/f noise. Contact noise, present in previous ac measurements, is avoided by utilizing a center-tapped, four-probe specimen geometry. Unlike the usual four-probe measurement this measurement is not sensitive to spatially correlated resistivity fluctuations such as those due to bath temperature fluctuations. The technique is generally applicable for specimen resistances $r < 10$ KΩ; we have used it to measure the 1/f noise of metal film conductors. Use of simultaneous direct and alternating currents provides new information that may be especially useful with non-linar conductors.

7. Acknowledgements

Most of this work was conducted in the laboratory and under the direction of W. W. Webb, with support from the National Science Foundation, both directly (DMR 8108328) and through the Materials Science Center (DMR 8217227-A01) and the National Research and Resource Facility for Submicron Structures at Cornell University. The author would like to thank R. F. Voss for initial suggestions that led to this technique, and K. Krafft, J. Mantese, and W. Webb for useful discussions.

References

1. Mark B. Ketchen and John Clarke, Phys. Rev. B 17, 114 (1978).
2. Gopa Sarkar De and Harry Suhl, Surface Science 95, 67 (1980).
3. M. R. Shanabarger, J. Wilcox, and H. G. Nelson, J. Vac. Sci. Technol. 20, 898 (1982).
4. M. Celasco, F. Fiorillo, and P. Mazzetti, Phys. Rev. Lett. 36, 38 (1976).
5. G. Bertotti, M. Celasco, F. Fiorillo, and P. Mazzetti, J. Appl. Phys. 50, 6948 (1979); also see Giorgio Bertotti and Fausto Fiorillo, in Noise in Physical Systems and 1/f noise, edited by M. Savelli, G. Lecoy, and J. -P. Nougier (North-Holland, Amsterdam, 1983), p.339.
6. John H. Scofield and Watt W. Webb, Phys. Rev. Lett. 54, 353 (1985).
7. Mark Nelkin, in Chaos and Statistical Mechanics, Springer Series in Synergetics, edited by Y. Kuramoto (Springer, Berlin, 1984).
8. P. Dutta and P. M. Horn, Rev. Mod. Phys. 53, 497 (1981).
9. J. W. Eberhard and P. M. Horn, Phys. Rev. Lett. 39, 643 (1977); also Phys. Rev. B 18, 6681 (1978).
10. J. H. J. Lorteije and A. M. H. Hoppenbrouwers, Philips Res. Repts. 26, 29 (1971).
11. H. Sutcliffe, Electron. Lett. 7, 160 (1971).
12. B. K. Jones and J. D. Francis, J. Phys. D 8, 1172 (1975).
13. B. K. Jones and J. D. Francis, J. Phys. D 8, 1937 (1975).
14. R. Rzemien, C. K. Iddings, and W. F. Love, Rev. Sci. Instrum. 50, 488 (1979).
15. H. Stoll, Appl. Phys. 22, 185 (1980).
16. C. Leemann, M. J. Skove, and E. P. Stillwell, Solid State Commun. 35, 97 (1980).
17. S. Demolder, M. Vandendriessche, and A. Van Calster, J. Phys. E 13, 1323 (1980).
18. Richard F. Voss and John Clarke, Phys. Rev. B 13, 556 (1976).
19. Seymour Letzter and Norman Webster, IEEE Spectrum 7, 67 (1970).
20. These noise figure contours were reproduced (with permission) from the operation and service manual of the Princeton Applied Research model 113 low noise preamplifier.
21. D. E. Prober, Rev. Sci. Instr. 45, 849 (1974).
22. Significant reduction of preamp noise by cross-correlation is time consuming. For instance, to reduce amplifier noise at 0.1Hz by 20 dB (factor of 10^2) requires averaging of $N = 10^4$ time records, each 20 seconds long; total time = 6 hours. See reference 17 for a description of the cross-correlation technique.
23. Conductivity fluctuations generally imply both resistive (δ=0) and reactive (δ=90 A) components due to Kramers-Kronig relations. Here we consider only conductors with a negligible imaginary component of the conductivity. See reference 14 for discussion of this.
24. In practice one of the standard plugin preamplifiers (PAR116, 117, 118) is used instead of the PAR113. Here the model 113 is used for direct comparison with the dc measurements.
25. John H. Scofield, Ph. D. thesis (Cornell University, 1985, unpublished).

26. John H. Scofield, Joseph V. Mantese, and Watt W. Webb, Phys. Rev. B 32, 736 (1985).

27. Closer inspection has always revealed macroscopic defects (such as film cracks, incomplete etching, etc.) that are probably responsible for any exceptions.

28. See Neil M. Zimmerman, John H. Scofield, Joseph V. Mantese, and Watt W. Webb, Phys. Rev. B 34, 773 (1986), and references therein.

29. D. M. Fleetwood and N. Giordano, Phys. Rev. B 27, 667 (1983).

30. Julius S. Bendat and Allan G. Piersol, Random Data: Analysis and Measurement Proceedures (Wiley, New York, 1971).

31. E. J. P. May and W. D. Sellars, Electron. Lett. 11, 544 (1975).

32. E. J. P. May and H. G. Morgan, Electron. Lett. 12, 8 (1976).

33. E. J. P. May and J. M. K. Horwood, in Proceedings of the Symposium on 1/f Fluctuations, Tokyo, Japan, 1977 (unpublished), p. 124.

34. B. K. Jones, Electron. Lett. 12, 111 (1976).

35. H. Sutcliffe and Y. Ulgen, Electron. Lett. 13, 397 (1977).

36. A. Kumar and W. I. Goldburg, Appl. Phys. Lett. 39, 121 (1981).

37. G. J. M. van Helvoort and H. G. E. Beck, Electron. Lett. 13, 542 (1977).

38. K. Krafft, unpublished, 1984.

Appendix A

Current Biased, Four-Probe Noise Measurement

The usual four-probe dc method for measuring resistance fluctuations is illustrated in Figure 1. We wish to calculate fluctuations, $\delta v = v - \langle v \rangle$, in the voltage v across the specimen resistance, $r \equiv r_1 + r_2$. It is assumed that the battery E_o and ballast resistors R_1 and R_2 do not fluctuate. Specimen ($\delta r \equiv \delta r_2 + \delta r_1$) and current contact ($\delta\xi_1$ and $\delta\xi_2$) resistance fluctuations contribute a component δv_I to δv,

$$\delta v_I = \bar{I}\,\frac{R'}{R'+\bar{r}}\left\{\delta r - \frac{\bar{r}}{R'}\delta R'\right\}$$

where $R_j' \equiv R_j + \overline{\xi_j}$ (j=1,2), $R' \equiv R_1' + R_2'$ is the effective ballast resistance, $\delta R' \equiv \delta\xi_1 + \delta\xi_2$ is the contact noise, $\bar{I} \equiv E_0/(R'+\bar{r})$ is the mean current, and $\bar{r} \equiv \bar{r}_1 + \bar{r}_2$, $\bar{\xi}_1$, and $\bar{\xi}_2$ are the mean specimen and current contact resistances respectively. (Note that in the limit as $\bar{r}/R \to 0$, the current $I \to \bar{I}$, and $\delta v_I \to \bar{I}\delta r$, i.e., the current does not fluctuate and there is no contact noise.) In addition to the above current noise (δv_I), Nyquist (or thermal) noise δv_N contributes to δv. The preamplifier also injects noise δv_A (as referenced to its input) so that the voltage δV at the preamplifier output is

$$\delta V = G\left(\delta v_0 + \delta v_I\right)$$

where G is the preamplifier voltage gain and $\delta v_0 \equiv \delta v_N + \delta v_A$ is the "background noise."

Assuming $\overline{\delta r \delta R'} = 0$, the power spectral density $S_V(f;I)$ of $\delta V(t)$ for a current I is

$$S_V(f;I) = G^2\left\{S_v^0(f) + \bar{I}^2\left[S_r(f) + \frac{\bar{r}^2}{R'^2}S_{R'}(f)\right]\right\}$$

where $S^o_V(f)$, $S_r(f)$, and $S_{R'}(f)$ are the power spectra of $\delta v_o(t)$, $\delta r(t)$, and $\delta R'(t)$ respectively. The background noise spectra $S^o_V(f) = G^{-2}S_V(f;I=0)$ is measured with zero current; current noise spectra are subsequently obtained from $S_V(f;I)$ by subtracting background. To distinguish $S_r(f)$ from $S_{R'}(f)$ it is necessary to determine the current noise spectra for two or more ratios ($\bar{r}/R'$).8

For comparison with the bridge circuit it is useful to define

$$\delta z_j \equiv \frac{R_j'}{R_j' + \bar{r}_j}\left\{\delta\bar{r}_j - \frac{\bar{r}_j}{R_j'}\right\}\delta\xi_j$$

for j=1 and 2, so that $\delta v_I = I(\delta z_1 + \delta z_2) \equiv I\delta z$. With these definitions the power spectrum $S_V(f;I)$ of the measured voltage $\delta V(t)$ is just

$$S_V(f;I)/G^2 = S_v^0(f) + I^2 S_z(f)$$

where $S_z(f)$ is the spectrum of $\delta z(t)$. For sufficiently large ballast resistors (i.e., as $\bar{r}/R \to 0$) $\delta z \to \delta r$ and $S_z(f) \to S_r(f)$.

The stability of the battery E_o and ballast resistors R_1 and R_2 may be determined by replacing the specimen with equivalent noise-free resistors (e.g., wire-wound) and measuring $S_V(f;I)$, both for zero current and for the maximum current to be used, I_{max}. The necessary stability in E is usually not achieved by power supplies. We have found the switch contacts of most decade resistors to be too noisy for use with continuous metal films.

Appendix B

Spectral Density Measurements With a Lock-in Amplifier

Recall that, in the five-probe bridge measurement, specimen resistance fluctuations (δr_2 and δr_1) modulate the bridge current to produce a bridge error signal $\delta v(t) = I(t)\delta r_-(t)$, where $\delta r_- \equiv \delta r_2 - \delta r_1$. Here we calculate the power spectral density $S_V(\omega)$ of the output of a lock-in amplifier for an input signal

$$\delta v(t) = \delta v_0(t) + i_0 \delta r_-(t) \sin\left(2\pi f_0 t + \delta\right).$$

The lock-in consists of an ac amplifier, a phase-sensitive detector (PSD), and a dc amplifier. The ac and dc amplifier stages are characterized by complex transfer functions $H_{ac}(\omega)$ and $H_{dc}(\omega)$. The PSD stage multiplies the time-domain output of the tuned amplifier by a square wave

$$e(t) = \frac{4e_0}{\pi} \sum_{n=1}^{odd} (1/n) \sin\left[n\left(\omega_0 t + \delta\right)\right]$$

of frequency $f_0=\omega_0/(2\pi)$, amplitude e_0, and fixed phase δ with respect to the carrier. The Fourier transform of the output voltage $\delta V(\omega) = \int_{-\infty}^{\infty} \delta V(t) e^{j\omega t} dt$ is

$$\delta V(\omega) = \frac{4e_0}{2\pi j} H_{dc}(\omega) \sum_{n=-\infty}^{odd} (1/n) H_{ac}(\omega + n\omega_0) \delta v(\omega + n\omega_0) e^{jn\delta},$$

where $j \equiv \sqrt{-1}$ and

$$\delta v(\omega) = \delta v_0(\omega) + \frac{i_0}{2j}\left\{\delta r_-(\omega - \omega_0) - \delta r_-(\omega + \omega_0)\right\}$$

is the Fourier transform of the input voltage. We consider only frequencies $f < f_0$ and assume $H_{dc}(\omega) = 0$ for $|\omega| \geq \omega_0$ (i.e., that the lock-in low pass filter is set to pass only frequencies below the carrier frequency). The power spectral density

$$S_V(\omega) \equiv \tfrac{1}{2\pi} \int_{-\infty}^{\infty} \overline{\delta V^*(\omega')\delta V(\omega)} d\omega'.$$

of the output voltage is

$$S_V(\omega) = \frac{\frac{e_0^2}{\pi^2}\left|H_{dc}(\omega)\right|^2 \sum_{n=-\infty}^{odd} (4/n^2)\left|H_{ac}(\omega + n\omega_0)\right|^2 S_v^0(\omega + n\omega_0)}{} + \frac{e_0^2}{\pi^2}\left|H_{dc}(\omega)\right|^2 \sum_{n=-\infty}^{odd} i_0^2 S_r^-(\omega + (n-1)\omega_0)\left[(1/n^2)\left|H_{ac}(\omega + n\omega_0)\right|^2 - \frac{e^{2j\delta}}{n^2 - 2n} H_{ac}(\omega + n\omega_0) H_{ac}^*(\omega + (n-2)\omega_0)\right],$$
$$+ \frac{e_0^2}{\pi^2}\left|H_{dc}(\omega)\right|^2 \sum_{n=-\infty}^{odd} i_0^2 S_r^-(\omega + (n+1)\omega_0)\left[(1/n^2)\left|H_{ac}(\omega + n\omega_0)\right|^2 - \frac{e^{-2j\delta}}{n^2 + 2n} H_{ac}(\omega + n\omega_0) H_{ac}^*(\omega + (n+2)\omega_0)\right]$$

where $S^-_r(\omega)$ is the power spectral density of $\delta r_-(t)$. The principal contribution to S_V comes from the $n = \pm 1$ terms (the only terms if the PSD multiplied by a sinusoid). Dropping higher order terms we find

$$S_V(\omega) \approx \frac{e_0^2}{\pi^2}\left|H_{dc}(\omega)\right|^2 \left\{ \begin{array}{l} 4\left|H_{ac}(\omega+\omega_0)\right|^2 S_v^0(\omega_0+\omega) + 4\left|H_{ac}(\omega_0-\omega)\right|^2 S_v^0(\omega-\omega_0) \\ +i_0^2 S_r^-(\omega)\left|H_{ac}(\omega_0+\omega)e^{j\delta} + H_{ac}(\omega_0-\omega)e^{-j\delta}\right|^2 \end{array} \right\}$$

.

Assuming a symmetric tuned amplifier, i.e., $H_{ac}^*(\omega_0+\omega) = H_{ac}(\omega_0-\omega)$, and $S_v^0(\omega_0+\omega) = S_v^0(\omega_0-\omega)$, we find that the one-sided power spectrum

$$S_V(f) \equiv 2S_V(\omega)\big|_{\omega=2\pi f}$$

is

$$S_V(f) = \frac{4e_0^2}{\pi^2}\left|H_{dc}(f)H_{ac}(f_0-f)\right|^2\left\{S_v^0(f_0-f) + S_v^0(f_0+f) + i_0^2 S_r^-(f)\cos^2(\delta)\right\}.$$

The transfer functions both become real and frequency independent as $f \to 0$. For sufficiently low frequencies the above equation becomes

$$S_V(f) \approx G_0^2\left\{S_v^0(f_0) + \tfrac{1}{2} i_0^2 S_r^-(f)\cos^2(\delta)\right\}$$

where

$$G_0^2 \equiv \frac{8e_0^2}{\pi^2}\left|H_{dc}(0)H_{ac}(f_0)\right|^2$$

is the square of the low frequency lock-in gain. With a carrier frequency f_o = 700 Hz, a tuned amplifier Q=1, and a single stage lock-in low pass filter time constant τ_D < 1 ms, these approximations introduce less than 1 dB error for f ≤ 50 Hz. Corrections for H_{dc} and H_{ac} extend measurements to 400 Hz. The error introduced by dropping higher order terms in the worst case (i.e., $|H_{ac}(\omega)|^2$ = constant, $S^-_r(\omega)$ = const.) is not more than 1 dB. To assure that H_{dc} is zero when $\omega > \omega_o$ the output of the lock-in's own low-pass filter is fed into a Unigon digital filter with a 120 dB/octave roll-off.